Journal of Materials Science: Materials in Electronics

CHAPMAN & HALL

JOURNAL OF MATERIALS SCIENCE: MATERIALS IN ELECTRONICS 6 (1995) 265–279

Review
Bulk growth of silicon–germanium solid solutions

J. SCHILZ
Institute of Materials Research, German Aerospace Research Establishment (DLR), Linder Höhe, D-51147 Köln, Germany

V.N. ROMANENKO
St. Petersburg State University of Architecture and Civil Engineering, 4, 2nd Krasnoarmeiskaya Street, St. Petersburg, 198005, Russia

This paper provides an overview of the technology for growing bulk silicon–germanium solid solutions and of the structural properties of the solidified materials. It is an attempt to summarize and value the methods and efforts applied to the controlled crystallization of silicon–germanium melts which were employed during the last four decades. The especially high degree of segregation makes the system sensitive to small changes of growth conditions, which leads to inhomogeneities and strain. The future availability of homogeneous, low-defect Si–Ge crystals through the whole composition range is briefly discussed.

1. Introduction

The Si_xGe_{1-x} solid solution has experienced a great resurgence since the discovery that strained Si–Ge/Si heterostructures offer the possibility to tailor the band structure of the alloy [1, 2]. This has reactivated great interest in investigations on the Si–Ge semiconductor system. However, thin strained layers are not a suitable system for the study of bulk fundamental properties relevant to device processing. There is a need to have bulk single crystals of this material available –Si_xGe_{1-x} crystals in a satisfactory quality over the whole composition range.

During the last four decades, bulk Si–Ge has been investigated mainly from a technological point of view. Emphasis was primarily put on performance problems of Si–Ge applications, e.g. in the field of photodetectors and thermogenerators (see Appendix). Therefore the studies on solidification behaviour, macro- and microsegregation effects were mostly superficial and what has been called a homogeneous crystal was more or less sufficiently homogeneous material for a certain application. Today, the possible applications of bulk Si–Ge crystals as substrates for layer structures pose higher requirements on homogeneity and crystallinity. This makes it necessary to go deeper into the technological and physical problems of Si–Ge solid solution solidification and to examine more carefully the questions on quality influencing effects, such as supercooling and phase stability.

As a first step towards the availability of low-defect single crystalline Si_xGe_{1-x}, this overview tries to summarize and evaluate the already applied methods and the derived results on Si–Ge solidification and aims to point out key open questions for further research.

2. The silicon–germanium solid solution

The complete mutual miscibility of the Si–Ge solid solution was shown by Stöhr and Klemm in 1939 [3] by casting a Si–Ge melt and repeated grinding and sintering. They found the substitutional solid solution structure, and their phase diagram is still the basis of the knowledge on the solidification behaviour of the material; only a few points have been later added to the Ge-rich side of the phase diagram [4, 5] (see Fig. 1). The large separation of the solidus and liquidus lines leads to critical solidification velocities on the order of mm/h (Section 4.1) and thus to long processing times. The high chemical reactivity of the molten silicon makes the system technologically difficult to handle (Section 3.7).

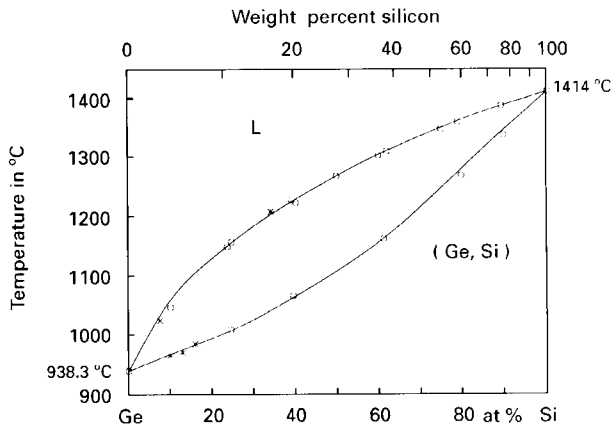

Figure 1 Si–Ge assessed equilibrium phase diagram. Redrawn after [5].

0957–4522 © *1995 Chapman & Hall*

3. Crystallization methods

All classical crystallization methods, such as zone melting, Czochralski and Bridgman method, and even vapour deposition have been applied in order to obtain homogeneous bulk Si–Ge crystals. Early attempts were made by slowly freezing a melt and it is reported that freezing Si–Ge with Si-contents below 12 at % leads to macroscopic single crystalline regions in the cm^3-range [6, 7]. The following sections will deal with controlled solidification methods focusing on the technology and the potential of the method to obtain homogeneous Si–Ge.

3.1. Float zone methods

The first method applied to the growth of Si–Ge single crystals was a horizontal float zone (FZ) recrystallization technique with the charge rod lying in a boat [8–14]. The authors found a very long initial transient of several cm, which is due to the low effective diffusion coefficient of Si in the melt. It was found that single crystalline material with Si-content less than 20 at % could only be grown at growth rates below 2 mm/h [10]. Single crystalline Ge was used as seed in this case. The macrohomogeneity of the solidified ingot was still not sufficient until the employment of the so-called (single pass) zone levelling method, where the starting zone consists of a composition $x_i = k \cdot x_c$ with x_c being the composition of the charge rod and k the segregation coefficient. Zone levelling avoids the initial transient and in [11, 12] the growth of homogeneous samples with Si-contents up to 50 at % are reported. Ingots, solidified at 3 mm/h, were claimed to be single crystalline (or at least twinned) for concentrations below 10 at % Si [11]. However, as no seeds were used, it is not convincing that the samples were real single crystals. The material is probably comparable to that obtained by a slow freezing procedure.

Larger temperature gradients at the crystallization boundary and concomitant, a better mixing of the melt and higher solidification rates with stable solid/liquid interface, can be achieved by a crucible free FZ method [15, 16]. Indeed, the critical solidification velocities were higher (Table I), but there was no success reported in obtaining single crystalline material above some at % Si in Ge.

So far the approach to the Ge–Si solid solution occurred from the Ge end of the phase diagram. The reason for this was the lack of equipment which is able to process material with much higher melting points. There was a report on FZ-solidification of Si-rich Si–Ge by Gurevich *et al.* [17], but it lasted another 15 years until the first single crystalline Si–Ge with a Si-content down to 65 at % was grown by employing FZ growth with electron beam heating [18]. This is a technique which results in even larger temperature gradients and critical growth rates (refer to Table I).

3.1.1. Travelling solvent method

An interesting FZ technique for obtaining homogeneous, but heavily doped semiconductors is the travelling solvent method (TSM). Here, an alloy is grown from a metallic solution with a much lower melting point than the mixture of the components alone. During the solidification, the metal is incorporated into the material up to its solid solubility and serves as a dopant [19]. TSM recrystallization of Si–Ge (80 at % Si) with Sn or Ga as solvent was performed at an extremely low speed of 0.4–0.5 mm/day [20]. Processing temperature in this case is only 800–900 °C, which allows the employment of quartz ampoules. In spite of the extreme low growth rate, solidification resulted in dense polycrystalline ingots with grain sizes of about 5–7 mm. Problems probably arise from precipitations of the solvent.

3.1.2. Starting material

A common problem of all float zone methods is the attainment of conditions of the starting zone and the charge rod which will yield macrohomogeneous material after one or several zone passes. There are some calculations, though not very precise and thorough, and experiments trying to forecast the composition of the Si–Ge starting zone and the profile of the feed rod [21]. Different thermal conditions between the middle and the ends of the rod were either compensated by varying the diameter of the feeding material or by using very short sample lengths.

In practice there are different approaches in preparing homogeneous feeding rods. For example by rapid cooling of a melt [22], by inserting a Ge bar into a Si rod [23], by inserting pieces of Si into a Ge rod (or vice versa) [10], or even producing stacks of alternating Ge and Si tablets [24]. Also sintered powder alloys were used [25]. The so-called Wacker process [13, 14], which was originally developed for producing Si–Ge for use in thermoelectric generators, can potentially be used for the production of homogeneous Si–Ge starting material. The principle is shown in Fig. 2. It consists in solidifying a Si–Ge melt in small portions in a crucible.

Typically such composite or granular materials undergo a homogenization process by floating with high speed. It is reported that a degree of macrohomogenization, sufficient for achieving single crystalline material by a final zone pass with low speed, can be reached by initial floating with 15 mm/h [26]. If crystals are directly grown from a charge rod consisting of Ge with an introduced piece of Si, the growth starts with pure Ge. And, when the Si piece is reached, a gradient in composition is built up. Stability studies found that monocrystals can be obtained if the gradients do not exceed 10 at %/cm [27, 18].

3.2. Czochralski method

The Czochralski (CZ) method has been extensively employed to obtain Si–Ge single crystals [28, 29, 30]. However, due to the continuous loss of Si during the solidification process, the growing crystal shows a non-constant concentration profile. The simplest method for minimizing this macrosegregation is growing small crystals from a large batch of melt, which is

TABLE I Experiments and results on growth rates of different Si–Ge compositions. (Remarks: X-ray: Debye-Scherrer X-ray photographs of ground samples or Laue back-reflection photographs of bulk samples; Metallography: Optical microscopy of etched samples; SEM: Scanning electron microscopy; EDS: Energy dispersive X-ray fluorescence analysis in SEM; TEM: Transmission electron microscopy; XRD: X-ray diffraction on bulk material rocking curves; HRXRD: High resolution X-ray diffraction on bulk material incl. Bond method and texture measurements.)

Experiments on growth rates of Si_xGe_{1-x}		Growth conditions			Results	
Reference	Method	Rate [mm/h]	Composition [at % Si]	Remarks	Analysis	Results
Mitrenin *et al.* (1957) [9]	Zone leveling	15.0	10	—	X-ray	inhomog.
		8.0	50	—		inhomog.
		7.5	10	—		inhomog.
		5.0	25	—		inhomog.
Belokurova *et al.* (1959) [31]	CZ with replenishment	102.0	0.7 to 2.0	Seed rot. 5 rpm, crucible 10 rpm, opposite sense	SEM, metallography	single crystal
Morton *et al.* (1959) [10]	Globar zone leveling	2.1	4.4, 7.5	—	Metallography	single crystal
Busch and Vogt (1960) [11]	HF zone leveling	3.0	10	—	X-ray, electr. resist.	single crystal
Selikson (1961) [28]	CZ	18.0	0.3	Seed rot. 5 rpm, crucible 10 rpm, opposite sense	SEM, metallography	single crystal
Nikitina *et al.* (1962) [62]	CZ with self replenishment	2.0	20, 30, 45	Seed rot. 2–60 rpm, crucible 9 rpm	X-ray	homogeneous
		10.0	- " -	- " -		inhomog.
		8.0	- " -	- " - incl. vibrat. mixing		homogeneous
Gurevich *et al.* (1964) [17]	HF float zone	60.0	91, 89, 87, 85	—	X-ray	inhomog.
		45.0	- " -	—		inhomog.
		24.0	- " -	—		inhomog.
Dismukes and Ekstrom (1965) [12]	Zone leveling	0.2	20, 30, 40, 50, 60	$G \approx 50$ K/cm	X-ray	homogeneous
		0.7	10, 50, 70	- " -		homogeneous
		1.6	10, 70, 80	- " -		homogeneous
		1.6	20, 30, 40, 50, 60	- " -		inhomog.
		3.2	40, 50, 70	- " -		inhomog.
		6.3	92	- " -		homogeneous
		6.3	70	- " -		inhomog.
Tairov *et al.* (1967) [22]	CZ with replenishment	2.5	15	—	Metallography	single crystal
		5.0	5	—		single crystal

TABLE I (Continued)

Experiments on growth rates of Si_xGe_{1-x}

Reference	Growth conditions				Results	
	Method	Rate [mm/h]	Composition [at % Si]	Remarks	Analysis	Results
Gromova (1968) [16]	HF float zone	84.0	up to 7	$G \approx 150$ K/cm (with cooler)	Absorption-spectroscopy	single crystal
Romanenko *et al.* (1970) [26]	Globar multipass zone leveling	13.0	18, 20, 30	—	X-ray, absorption-spectroscopy	inhomog.
		15.0	30	—		inhomog.
		20.0	20, 25	—		inhomog.
		0.98	10, 15, 20, 30, 90	—		homogeneous
Siethoff (1971) [64]	Float zone	90.0	99	Seed rot. 5 rpm	Metallography	single crystal
Dismukes and Yim (1974) [59]	Zone leveling	19.0	5	—	X-ray	homogeneous
Dolivo-Dobrovol'skaya and Smirnov (1975) [51]	CZ	30.0	4	$G \approx 5$ K/cm	Metallography	single crystal
		3.0	20	- " -		single crystal
Saidov and Umerov (1978) [24]	E-beam float zone	12.0	$\geqslant 88$	Rot. of rods	Metallography	single crystal
		12.0	75	- " -		inhomog.
Saidov *et al.* (1978) [61]	E-beam float zone	18.0	84	Rot. of rods	Metallography	single crystal
		12.0	75	- " -		single crystal
Kimura *et al.* (1981) [29]	CZ	0.5	88	Seed rot. 8–10 rpm, crucible 6–20 rpm	SEM, EDS, X-ray	single crystal
Saidov *et al.* (1981) [18]	E-beam float zone	3.0	65	Rod rot. 0.083 and 0.033 rpm, respectively	Metallography, X-ray	single crystal
		6.0	70			single crystal
		12.0	75			single crystal
		18.0	80			single crystal
Tairov (1966) [33] (1983) [21]	CZ with replenishment	2.5	0 to 15	Seed rot. 15 rpm	Density, metallography	single crystal
		$\geqslant 3.0$	0 to 15	- " -		polycrystal
Rouzaud *et al.* (1985) [38]	Vertical Bridgman	3.0	5	$G = 55$ K/cm, without seed	SEM, EDS	homogeneous
Kilmer *et al.* (1991) [25]	HF zone leveling	1.8	80	$G \approx 110$ K/cm	SEM, EDS, TEM, X-ray	single crystal
Dahlen *et al.* (1994) [40]	Vertical Bridgman	0.6	15	$G \approx 35$ K/cm	metallography, XRD	single crystal
Dahlen *et al.* (1994) [40]	CZ	2.8	8.8	Seed rot. 5 rpm	metallography, XRD	polycrystal
		2.4	27	Seed rot. 40 rpm		polycrystal
		7.6	89	- " -		single crystal
		60.0	99.5	- " -		single crystal

TABLE I (Continued)

Experiments on growth rates of Si_xGe_{1-x}

Reference	Growth conditions				Results	
	Method	Rate [mm/h]	Composition [at % Si]	Remarks	Analysis	Results
Kürten and Schliz (1994) [30]	CZ	3.0	98	Seed rot. 10 rpm, no crucible rot.	HRXRD, SEM, EDS, metallography	single crystal
		2.0	95	- " -		single crystal
		1.0	92	- " -		single crystal
		1.0	91	Seed rot. 5 rpm		single crystal w. striations
		0.7	90	Seed rot. 20 rpm		single crystal
		0.7	90	Seed rot. 5 rpm		single crystal w. striations
		0.5	85	Seed rot. 20 rpm		single crystal
		0.4	79	- " -		single crystal

Figure 2 Principle of Wacker process for obtaining macrohomogeneous, polycrystalline Si–Ge rods.

not an economic method and therefore only applicable for laboratory experiments. An elegant, but difficult technique is a melt feeding procedure, where the Si loss is replenished by a controlled feeding of a homogeneous Si–Ge rod (similarly prepared as the feeding rods used in FZ) into the melt [22, 31, 32, 33]. In the Russian literature this technique is named Petrov's method [34], and in principle it is equivalent to a float-zone method with a crucible [35, 36]. The advantage of CZ growth with replenishment compared to float zone growth is the absence of difficulties with zone length and zone stability. On the other hand there are problem with impurities picked up from the crucible.

A constant melt composition can also be achieved by the so-called self-feeding method, where the melt is placed into a crucible made of the higher melting component, which in our case is Si. Keeping the solidification temperature constant allows the dissolving of exactly that amount of Si which is lost by segregation [37]. The most difficult problem of this method is the requirement of a constant temperature field. Especially during the seeding process the necessary superheating changes the melt composition. Also during the growth, the temperature is a function of the sample length and sample diameter. Grown ingots are reported to have a high degree of macrohomogeneity, but they were all polycrystalline.

3.3. Bridgman method

In contrast to the CZ-method, directional solidification, i.e. mostly the Bridgman process, can handle only a small melt volume, since heat flow should always be perpendicular to the phase boundary. Because of this technical problem, and due to the

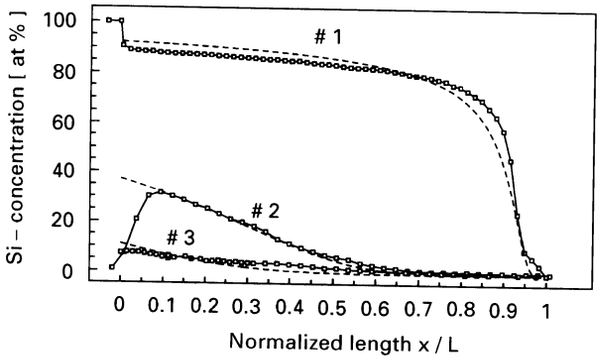

Figure 3 Segregation profiles obtained after directional solidification of three different Si–Ge melt compositions. Sample no. 1 was solidified with a Si-seed and samples 2 and 3 were seeded with pure Ge. (– – –) Calculation: complete mixing. (–□–) EDX measurements.

inevitability of the non-uniform composition profile after solidification, the Bridgman method has neither been applied for the growth of technically exploitable Si–Ge semiconductor material, nor was it subject to intense research in this field, in spite of the fact that a gradient in composition offers a new degree of freedom in tailoring devices (ref. to the appendix). Obtaining graded composition material, however, requires control of the segregation profile, which in turn requires the knowledge of parameters such as convection states. In the case of Si–Ge, the temperature and the solute field result in density gradients which influence natural convection in the crucible. Experiments suggested that in bottom-seeded vertical Bridgman growth, the damping power of the solute field is predominant over the thermal influence. Observed segregation profiles exhibit a typical diffusion controlled shape [38–40]. The experiments were performed with Ge-rich material and the thickness of the δ-layer in front of the phase boundary was found to be larger than the characteristic length D/v (D diffusion constant, v solidification velocity), which, in the present case, has a value of 3 cm. On the other hand, recent investigations revealed segregation curves close to those expected under the assumption of complete mixing of the melt [41], though the solidified samples had similar shapes and compositions to those in [38]. Segregation curves obtained are shown in Fig. 3 and will be discussed in Sections 3.5 and 3.6.

3.4. Vapour growth

Due to the low growth velocities, the production times of Si–Ge become so long that even vapour transport methods are taken into account to grow bulk material. Growth from vapour is even advantageous for the reason that the growing crystals are uniformly tempered and bathed in a uniform atmosphere. Thus homogeneous material is to be expected.

One type of vapour growth technique applied to Si–Ge is the sealed tube chemical transport method using either selenium [45], bromine [46] or iodine [47] as transport agent. The growth was performed without seeds over the whole composition range. Material grown by Se transport at temperatures between 1000 and 1250 °C and Se vapour pressure of 13 to 15 atm, was reported to be monocrystalline or at least twinned. The use of Br resulted only in polycrystalline growth. However, even the material considered to be monocrystalline did not consist of grains larger than several mm^3.

Another vapour growth method is a low pressure chemical vapour deposition procedure (LPCVD) from a gas-mixture of monosilane and monogermane [48]. Compared with the efforts needed to regulate the composition of a melt by feeding rods etc., the constitution of the atmosphere and thus the composition of the growing crystal is much easier to control. Yield, however, is still smaller than by melt processing, but vapour deposition is interesting for producing special types of crystals. For example the possibility of obtaining material with nearly any composition profile was exploited to prepare gradient Si–Ge crystals used for thermal neutron diffractometer applications [49, 50]. Growth of material roughly 1 mm thick on Si–substrates at a growth rate of 1 mm/day was shown to be possible.

3.5. Gravity effects

A strongly segregating system is extremely sensitive to any change in growth parameters, and is therefore a good sensor for the investigation of convection states. As most types of convections are gravity driven, a thorough study in this field requires growth under different gravity conditions, which, in the simplest case, can be achieved by changing the growth direction in respect to the g-vector. Real gravity enhancement can be obtained by e.g. conducting experiments in a centrifuge. More difficult is the attainment of reduced gravity, which requires free falling solidification furnaces or the growth of crystals onboard a spacecraft. Though the Si–Ge solid solution is proposed to be an appropriate vehicle for investigating the influence of gravity, up to now there have been only some more or less preliminary studies or sporadic outcomes about the influence of gravity on the segregation behaviour.

A gravity driven segregation in horizontally zone levelled samples was already mentioned in 1965 [12]. The solidified ingots showed an increase in Ge content from the top to the bottom. The 50-50 Si–Ge samples showed the largest de-mixing effect. The explanation is obvious since the concentration difference across the boundary layer is least for dilute alloys and exhibits a maximum somewhere in the middle of the phase diagram. This would indicate that gravity indeed has an influence on mixing or de-mixing of a solid solution with constituents differing considerably in density. A similar effect was observed during the comparison of upward and downward solidified FZ samples [18]. Ingots floated opposite to the g-vector contained more Ge in the first part of the sample than in the other case. This means that an upward travelling interface reduces the effect of natural segregation. If it is solidified in the opposite direction, the heavy Ge-component travels away from the liquid/solid

interface, thus Si-rich material is left at the interface. At the same solidification distance, the concentration profiles differ up to 10 at % between upward and downward growth at average sample compositions of 60 at % Si. If bottom seeding is used, the axial concentration and temperature fields damp the flow. Indeed the material by downward FZ technique showed more nucleations than in the opposite case, which indicates more pronounced convection driven composition fluctuations near the phase boundary [18].

The results derived from the FZ solidification experiments support the findings of diffusion controlled segregation profiles during directional solidification [38–40]. In spite of the rather slow processing speed, it seems that the mixing of the melt is not complete. Recent vertical Bridgman experiments, however, revealed segregation profiles, which only can be explained by the assumption of a completely mixed melt [41]. Since vertical Bridgman is a thermally and solutally stabilizing setup, thermal and solutal Rayleigh numbers are less than zero and melt flow is mainly driven by radial temperature gradients. Thus the possible mechanism responsible for the contradictory results can only be found in different radial temperature variations. In [41] the deflection of the phase boundary is equivalent to a radial temperature gradient of about 20 K/cm whereas in [38] radial temperature gradients between 2 and 7 K/cm are reported. Employing a model that compares the flow speeds (in respect to growth velocity) of the two situations, one finds that in the first case concentration differences are washed out quickly and the flow is driven by the thermal field only. If the radial temperature gradient is as low as in the latter case, it is possible to build up a concentration gradient, which in turn stabilizes the situation by damping the flow. The reduced convection allows a larger diffusion boundary layer. This suggests that the flow intensity, which is driven by a horizontal temperature gradient in a thermally and solutally stabilizing configuration makes a transition when the horizontal thermal Rayleigh number changes from 150 (diffusion controlled) to 610 (complete mixing).

There are some experiments on Si–Ge which have been performed under microgravity conditions. A Si–Ge crystallization experiment took place onboard the coupled Soyus-Apollo spaceships [42–44]. Homogeneous, single crystalline Si–Ge–Sb rods prepared by CZ with replenishment containing 1 at % Si and 0.01 at % Sb were partly remelted in a closed ampoule. Growth was performed at the quite high speed of 22 mm/h in a furnace with a temperature gradient of only 10 to 12 K/cm. Results of this enterprise are reported as following: The initial transient of the solidified ingots showed a small increase in Si-concentration, which was thought to be in contrast to all accepted segregation theories. In addition, a pronounced compositional inhomogeneity within the cross sections of the samples were found. The two solute components accumulated at opposite sides of the samples. No explanations or attempts thereof were given for these phenomena. Our interpretation of the initial increase in silicon is the transient which is found if a lower melting Si–Ge mixture is used as seed. This will be discussed in the following section.

3.6. Seeding

Growth of Si–Ge can either start from pure Ge or Si seed crystals. However, due to the large variation in melting point with composition, the system does not tolerate large differences in the composition between seed and grown crystal. (The difference in lattice constant does not play the major role in this case. Strain originating from a lattice mismatch will be released by the production of dislocations as shown in Section 4.3.) The growth of Si–Ge starting from pure Si – i.e. with a seed which has a higher melting point than the grown crystal – was found to be easier than proceeding from the Ge-rich side. As the previous sections showed, all authors beginning with pure Ge ended up with Si–Ge containing not more than a few percent silicon. When the melt is seeded with a material having a lower melting point than the developing crystal, the dissolved portion of the seed will be carried away, which leads to an increase of material with higher melting point than the actual temperature in front of the interface. This will induce an uncontrolled solidification with a rate generally faster than the critical growth velocity which finally results in polycrystalline growth [41]. Curves no. 2 and 3 in Fig. 3 clearly show the initial transient that forms with pure Ge as seed.

On the other hand, with pure Si as seed, it was found that CZ Si–Ge down to compositions of 90 at % Si can be grown without considerable matching problems [29, 30]. A closer observation of the remelt boundary shows that a transient region from pure Si down to the mixed crystal composition has been formed (see also curve no. 1 in Fig. 3). The growth remains stable and though the transition length is only on the order of ten micrometers, the graded link does not lead to polycrystallinity in CZ growth of Si–Ge. Only when the step approaches 15 at %, the interface becomes rough on a length scale of several micrometers, which has been often found to act as a source for twinning.

Also diameter changes during the growth were found to induce twinning [51, 29, 30]. Thus it is necessary to hold diameter variations of the growing crystal as small as possible. Especially the usual necking procedure has to be avoided. Another source of defect formation occurring when the crystal is pulled from the melt, is a polycrystalline peripheral layer that forms when the melt creeps up the grown material and solidifies in an uncontrolled manner [18, 52].

3.7. Crucible materials

Molten Si is very reactive to almost every known material. When Si–Ge is grown from a crucible, the solidifying melt adheres to the container wall and, due to the different thermal expansion coefficients, the ingot or the container is likely to crack. This may be dangerous, especially when repeated melting and solidification is required.

Quartz crucibles are commonly used for CZ-processing of Si and cause the least problems in terms of

purity. In CZ-growth, solidified crystals do not have any contact to the container and the unavoidable cracking during the cooling phase does not pose any difficulty. This makes quartz the material of choice for Si–Ge CZ growth. Also for zone melting/leveling [9, 25] of all Si–Ge compositions or Bridgman growth of Ge-rich material [38, 40], the use of quartz boats and ampoules, respectively, is reported. By using extremely slow cooling rates, cracking of containers or ingots could be mostly avoided – however, a reaction between crystal and ampoule was still detected and identified as a source for polycrystalline growth. Only when Si–Ge is grown from metallic solutions with a melting temperature below 900 °C [19], can quartz ampoules withstand the melt.

The classical crucible material for Ge-processing is carbon. Pure Ge does not wet carbon, but a Si–Ge melt containing only a small amount Si (say 1 at %) will stick to and react with a carbon vessel forming SiC. Even vitreous carbon with its smooth surface reacts with a Si–Ge melt. There are reports on the use of carbon boats for zone melting [9] and for Bridgman growth of Si–Ge with low Si content [38], but for defect generation the same holds true as in the case of quartz ampoules.

A material proven to be inert against Si is boron nitride (BN) [53]. Mostly hot-pressed BN is used, but due to the volume expansion of Si–Ge during solidification, the grown ingot is always indented with the rough surface of the BN crucible. A better choice is pyrolytic BN. Its smooth surface exhibits a high degree of chemical inertness [54] and for Si contents below 40 at % there is little adherence to the crucible wall and thus no difficulty in removing the ingot from the ampoule tube [55, 41]. A disadvantage of BN crucibles is the dissolution of boron into the melt. Processing in BN ampoules leads to p-type crystals with a density of electrically active impurities around 10^{16} cm^{-3}.

A different approach in obtaining suitable crucible material is to cover quartz with a thin layer of inert material which prevents wetting by the melt. Oxides, such as BeO, ZrO_2, and ThO are recommended [10, 11, 26, 56] and BeO is said to show the best performance. However, there are problems with toxicity. ZrO_2 and BN coating [57] are second in choice.

4. Structure and composition of crystals

This section is about the component distribution and the resulting structure of Si–Ge single crystals. It covers the range from macroscopic phenomena such as critical growth velocity and segregation coefficients down to investigations of germanium and silicon distribution on an atomic scale. There is still the contentious issue of the existence of superstructures in the Si–Ge solid solution.

4.1. Growth rates

Based on Tiller's criterion [58] the critical growth rate, v_c, for Si–Ge as a function of the composition has been numerically computed [59], taking the composition dependent segregation coefficient, k, and linear interpolated diffusion constants, D, into account (self diffusion coefficients: $D_{Ge} = 6 \cdot 10^{-5}$ cm^2/s, $D_{Si} = 3 \cdot 10^{-4}$ cm^2/s; hence $D_{Si\,Ge} = (30\text{–}24\ x) \cdot 10^{-5}$ cm^2/s). The v_c-values are calculated to several mm/h and the authors showed that the simple Tiller model is sufficient enough to compare with experimental results. More sophisticated approaches, as Mullins-Sekerka-modelling, lead to critical growth rates about 50% higher than those predicted by the Tiller model. Mullins-Sekerka theory gives the additional result of the wavelength of distortions at the onset of instability [60], but up to now there is no published experimental work about this subject.

We recalculated $v_c(x)$ according to [59]. The result is shown in Fig. 4 for two different temperature gradients, G. The most uncertain parameter in the calculation is the slope of the liquidus curve. At both ends of the Si–Ge phase diagram an error of factor 2 is likely to occur. Various experimental data points from different authors are included in Fig. 4. As the individual G-values are mostly unknown, v_c is drawn as a band covering a range from 25 to 50 K/cm. The experimental data, which are also listed in Table I, are drawn as full symbols when homogeneous/single crystalline material was grown, and as open symbols for inhomogeneous growth, distinguishing crystals solidified with stable liquid/solid interface from those where the phase boundary was unstable and thus constitutional supercooling occurred.

On the Ge-rich end the shaded area indeed serves as demarcation line for stable/unstable growth. On the Si-rich end, however, much larger solidification velocities were experimentally observed. This might be due to the application of growth procedures with much higher gradients in the melt than usual, e.g. electron beam FZ technique [61, 18]. There are some data points falling out of the validity of the model, i.e. [62]. Here, effort was made to destroy the δ-layer in front of the phase boundary by applying vibrations to the pulling system of the CZ-equipment [63], which leads to higher pulling speeds than predicted by the model. The method, however, did not deliver single crystals.

4.2. Segregation coefficients

The segregation coefficients derived from the phase diagram, k(x), determine the crystal composition for conditions without any pile-up of solute at the phase boundary. This condition may be achieved for small solidification velocities. Figs 5(a and b) plot the equilibrium distribution coefficients k_{Si} and k_{Ge}, respectively, as a function of crystal composition (solid lines). Of practical importance is the knowledge of the distribution coefficient under the conditions of a specific growth method, i.e. the effective segregation coefficient, k_{eff}, which is in general a function of many parameters, especially solidification velocity, v, and mass flows in the melt.

For the particular method of the CZ-process, k_{eff} has been determined as a function of composition

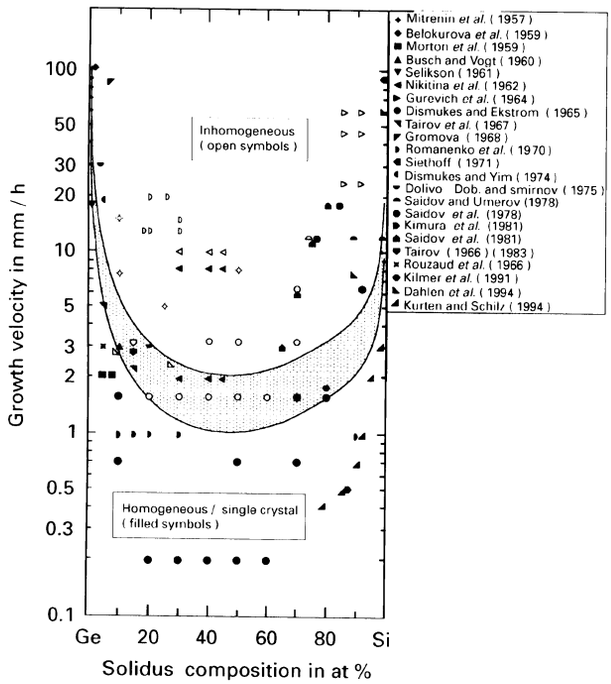

Figure 4 Si Ge growth rates as a function of composition: Full symbols denote growth of homogeneous/single crystalline material; open symbols stand for solidification with unstable solid/liquid phase boundary. Solid curve shows computed critical growth rates for a gradient range between 25 and 50 K/cm.

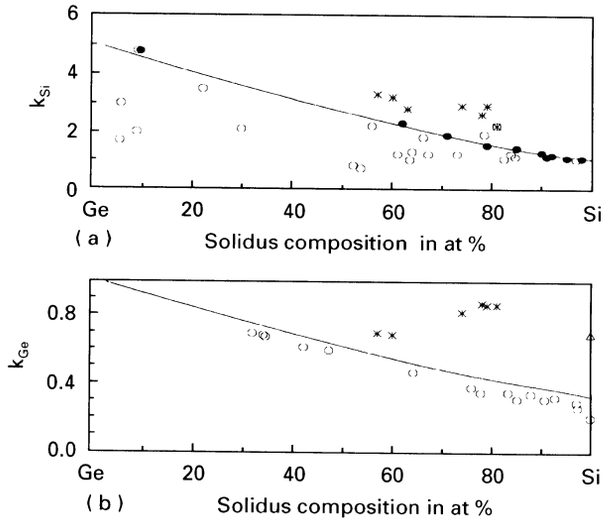

Figure 5 Segregation coefficients of Si Ge as a function of crystal composition. (a) Si in Ge and (b) Ge in Si. Solid line: Equilibrium segregation coefficient derived from the phase diagram. Symbols: Experimental data points. (Note that the abscissae show the composition of the solidified crystal

[30, 65, 66, 67, 68, 69]. For Ge concentrations below $1.5 \cdot 10^{20}$ cm^{-3} (which in fact are doping concentrations) a value of $k_{eff,Ge} = 0.68 \pm 0.05$ was found [67]. Within the mentioned uncertainty of factor two this might be identical with the equilibrium value of 0.32, but as the applied pulling speed had a rather high value of 50 to 100 mm/h, no final answer can be given. In [65] k_{eff} was determined over the whole composition range of Si–Ge and it was stated that there is virtually no difference between k_{eff} and k for solidification velocities below 3.6 mm/h. Symbols in Fig. 5 mark the experimental effective k-values by the different authors. k_{Si}-values from [65] are systematically lower than the equilibrium ones and one might think of an influence from the boundary layer. On the other hand the segregation coefficients for Ge from the same paper are almost identical with the equilibrium values. The discrepancy is probably due to systematic errors in the spectrochemical analysis and due to the fact that values for k_{Si} and k_{Ge} were determined from different sample batches.

As discussed in section 3.1 the mixing of the melt in electron-beam FZ Si–Ge growth [18, 70] was obviously worse than usual. This also manifests in a non-negligible dependence of k_{eff} on solidification velocity in the mentioned case. The equilibrium value seems to be reached only at velocities below 1 mm/h [71].

Though there is substantial scatter in the experimental data for k_{eff}, segregation values derived from the phase diagram can be used to calculate the melt composition for obtaining a desired Si/Ge ratio in the grown crystal in cases where the mixing of the melt is sufficiently effective, e.g. in CZ growth. The observed consistency allows the reverse conclusion that the Si–Ge phase diagram can be regarded as verified by a method independent from the usual calorimetric measurements.

4.3. Microsegregation and defects

The composition of the grown crystal is a function of the δ-layer extent in front of the solid/liquid interface. For example in Si–Ge CZ-growth the extent of this layer is estimated to be on the order of 0.1 mm; not exceeding 1 mm [66, 40]. A value directly calculated from the initial transient when a higher melting seed is used, suggests an even smaller value of 15 μm [41]. Any change in the thickness of this diffusion zone leads to compositional fluctuations, e.g. striae in the solid, which were often observed in practice [12, 30, 40, 41]. There are some works reporting a striation spacing of 10 to 15 μm, which was found to be independent of the growth method, i.e. zone levelling, CZ, or Bridgman, and independent of growth rate, composition, and temperature field. In [12] it was tried to connect the pattern with the observed temperature fluctuations, but no data are given to compare with the results.

In Fig. 6(a) a CZ grown $Si_{0.9}Ge_{0.1}$ crystal with the mentioned striation fine structure (amplitude 0.6 at %) of about 10 μm is shown. Growth direction is from top to bottom with a speed of 10 mm/h, a value already above the calculated critical value of only 4 mm/h (compare Fig. 4). In spite of this high speed, the interface in the upper region where the crystal was grown without rotation, is nearly undistorted. Only when the rotation is switched on, distorted, but still not polycrystalline, growth starts. Switching the rotation off again during this stage of disturbances, will lead to a recovering of the planar phase boundary. In Fig. 6(b), where the local growth velocity is even larger (the distances between the rotational striations appearing every 30 s give values around 15 mm/h), another mechanism of distortion reversibility can clearly be seen: The inclination of the phase boundary

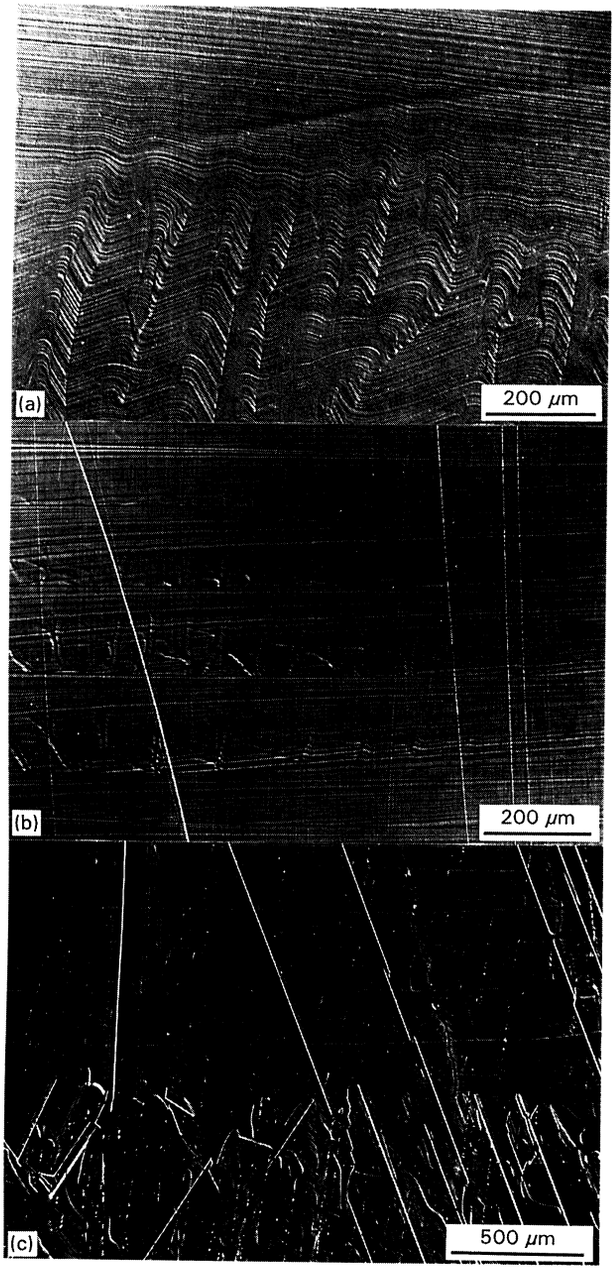

Figure 6 CZ growth $Si_{0.9}Ge_{0.1}$ crystal. Growth direction downwards. (a) Growth velocity 10 mm/h without seed and crucible rotation in the upper part and with seed rotation in the lower. (b) Local growth velocities around 15 mm/h. Distortions are periodically annealed by remelting. (c) Polycrystalline growth at 15 mm/h (upper part) and 30 mm/h (lower part).

modulates the local growth velocity in the way that between two striations a critical value is exceeded, which induces the observed defect structure. Though the distorted growth proceeds for more than 50 μm, an annealing of the interface occurs when the next growth striation remelts a portion of the solid [72]. A conclusion can be drawn from these microscopical observations that the Si–Ge system tolerates much larger solidification velocities than predicted and the growth with a planar interface presents a stable condition for the system even when it occurs at a speed three or four times larger than calculated for the onset of constitutional supercooling. Part (c) of Fig. 6 shows real polycrystalline growth of a Si–Ge crystal. If distorted growth as in Fig. 6(a) continues at a solidification speed of 15 mm/h, the structure develops twin boundaries (white lines in the photo), and if the growth velocity is even raised to 30 mm/h as in the lower part of (c), the grain structure becomes more pronounced.

There is only one published work dealing with the transition from monocrystalline to polycrystalline growth shown above. Investigations were performed by carrying out texture measurements connected with EPD determinations performed on FZ Si–Ge [73]. The only reported result was a correlation between the degree of disorientation and the density of etch pits.

There are several other mechanisms which have been identified to induce defect structures. It was found that twins start to develop if the crystal diameter exceeds 6 mm [51]. A similar effect was observed if the diameter undergoes excessive changes [30]. Another origin of twin formation was already mentioned in Section 3.6, where a polycrystalline wetting layer may induce misorientations in the growing crystal.

Dislocation densities in Si–Ge solid solution single crystals were found to lie in the range between 10^3 and 10^7 cm^{-2} [18, 74, 75]. Typically the EPD in the center of grown crystals is one or two orders of magnitude lower than on the periphery. In [75] it was shown that the structural defect density of Si-rich Si–Ge is nearly an exponential function of the Ge-content. Defect density rises from 10^5 cm^{-2} for material with 1 at % Ge up to 10^7 cm^{-2} for Si–Ge containing 20 at % Ge.

Arrays of dislocations lined up parallel to growth striae have been observed [76, 64]. Obviously the compositional fluctuations and thus fluctuations in lattice constant cause strain that has to be relieved. The authors estimate that already a concentration step of 0.1 at % will produce a linear dislocation density of about 1000 dislocations per cm. Only when the solute content (either Ge or Si) is decreased below 0.5 at %, periodic variations are reduced in height and misfit dislocations are no longer required to accommodate the diminished internal stresses [77]. As the center of a crystal is more inert against temperature changes than the periphery, the amplitudes of striations are much lower, which leads to the observed lower defect density. If it is possible to grow large diameter Si–Ge, material with defect densities below 10^3 cm^{-2} should be possible.

4.4. Microscopic ordering

There is still a debate, whether the Si–Ge substitutional solid solution possesses any long or short range ordering, i.e. the existence of any ordered structures is still open to question.

4.4.1. Energy of mixing

The discussion originated in a number of publications by Soma [78, 79, 80, 81], who calculated the energy of mixing of a Si–Ge solid solution. From the experimental phase diagram he found that the

interaction parameter, Ω, which is defined by $\Delta E_m(x) = \Omega x(1-x)$ with E_m being the energy of mixing, has a positive value of about 4 kJ/mole. The existence of a positive ΔE_m leads to the consequence that at absolute zero temperature a solid solution Si–Ge does not exist. Instead, atoms will be arranged as a mixture consisting of two phases, forming clusters of pure Ge and pure Si. At finite temperatures there is still a tendency to segregation. Up to a certain temperature, depending on the numerical value of Ω and the volume contraction [82] during the formation of the solid solution, a phase mixture of a Ge-rich and a Si–rich phase is more stable than a solid solution.

Though the behaviour of possessing a positive energy of mixing is quite common in solid solutions [83, 84], these initial results attracted others to perform more sophisticated calculations for Ω or for the critical temperature up to which a phase separation occurs [82, 83, 85, 86, 87, 88, 89]. The values for Ω scatter around 7 kJ/mole and the highest critical temperature reported was 360 K [88], which was obtained by applying a microscopic theory to the Si–Ge atomic structure.

The fact that a phase separation might occur to lead an extensive search for experimental evidence. Diffuse X-ray scattering has been performed on melt grown crystals [84, 90, 91]. The results indicated that in the vicinity of an atom there is an excess of atoms of the same kind. The tendency to form clusters presents a certain kind of short-range ordering. Similar conclusions were drawn during the evaluation of electric transport measurements performed on gallium doped Si–Ge [92]. The temperature dependence of the conductivity suggested the existence of a hopping process, which leads to the conclusion that Si atoms form clusters in the Ge–matrix. The cluster size was estimated to lie between 30 and 150 atoms, i.e. agglomerations with a typical radius of 2 to 3 nm.

4.4.2. Atomic structure of Si–Ge

A positive energy of mixing implies the existence of a short-range order in Si–Ge solid solutions. Si-rich and Ge-rich regions might form. Underlying this picture is the tacit assumption that Ge and Si occupy lattice sites only according to their probability of occurrence, i.e. Si–Ge behaves as a complete random solid solution. However, it is not excluded that a long-range ordering exists, where a superstructure in the Si–Ge lattice is formed by a regular occupation of the lattice.

Determinations of crystal binding energies of an equiatomic Si–Ge mixture or solid solution, based on pseudopotential calculations [93], revealed that the total energy favours a Si–Ge mixture over a random sited solid solution, and the disordered solid solution in turn, is favoured compared to a zinc-blende superstructure. On the other hand there is a study on the binding energies of the Ge 3d and Si 2p core electrons by X-ray photoelectron spectroscopy (XPS) [94], which found that there is virtually no dependence on

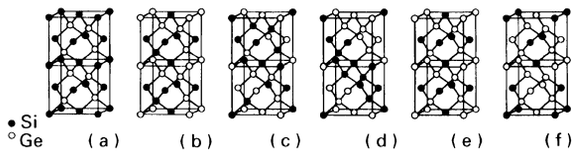

Figure 7 Possible ordered structures of an equiatomic Si Ge semiconductor alloy. Structure (d) was experimentally observed.

composition. This indicates that the electronegativities of Si and Ge are almost equal, from which we can conclude that ordered structures (e.g. zincblende long-range ordering for a 50–50 solid solution) are not energetically favoured. The statement of the absence of any long-range order is confirmed by Monte Carlo simulations on the equilibrium structure of Si–Ge [95]. However, these theoretical considerations predicted the absence of any short-range order as well, with the conclusion that Si–Ge behaves like a regular solution.

In contrast to this, a microscopic model for the binary Si–Ge [88] reveals that the formation energy for ordered structures is somewhat lower than for the complete random solution, which means that a long-range ordering is *indeed* energetically favoured. Types of possible superstructures for an equiatomic alloy are displayed in Fig. 7. The energy difference is only small – e.g. for zincblende (structure (a) in Fig. 7) the energy of mixing is $\Delta E_m(0.5) = 0.9$ kJ/mole, compared to 1.1 kJ/mole for disordered equiatomic Si–Ge. There is additionally a statement that the Si–Ge heteropolar bond is weaker than the average of the two homopolar bonds, and hence the rhombohedral structure (c) in Fig. 7 with 75% heteropolar bonds is even more stable than the zinc-blende structure with all bonds being heteropolar [87]. Thus it might be that during crystallization of Si–Ge, long-range ordered structures are preferred rather than the formation of a complete random sited lattice.

The existence of long-range ordered structures have been experimentally verified by selected area transmission electron diffraction (SAD) of Si Ge layers on Si-substrates [96]. Strain as a possible origin was excluded. The material was essentially bulk. The observed diffraction patterns are consistent with structures (c) and (d) in Fig. 7, but the authors considered only the CuPt type structure (c). Another work found similar superlattice diffraction patterns of unstrained equiatomic Si Ge layers [97]. Their superlattice signals were very strong making it possible to determine that only structure (d) can explain the observed patterns. It was noted that structure (d) has only 25% Si Ge bonds and should be even more stable than the rhombohedral structure (c) with 75% heteropolar bonds. These findings were later confirmed [98] and it was found that the investigated samples showed a reversible ordered/non-ordered phase transition at about 800 °C.

Thus it seems that there is indeed an occurrence of ordered structures, which certainly do not originate from strain. Though there is a difference in processing temperature between bulk-like layer material and melt

grown bulk crystals, the existence of superstructures (e.g. for an equiatomic solid solution type (d) in Fig. 7) is not excluded. If the difference in total energy between a long-range ordered Si–Ge alloy and that of a disordered solid solution is large enough, it should be reflected in physical properties, as band gap etc. Such investigations have not been performed up to now in Si–Ge.

5. Conclusions

To date single crystalline Si–Ge mainly represents a solid solution used for laboratory research. The large degree of segregation makes it sensitive to any change in growth parameters thus providing an interesting system for the study of solidification and crystallization processes. The continuous change of many physical parameters of Si Ge as a function of composition and the transition point in band-structure at 15 at % Si (see appendix) also make the solid a fascinating matter for research.

There is indeed a potential for technological applications, but the low solidification rate as a necessary condition for single crystalline, homogeneous growth, poses a limitation on the output of material. Therefore methods have to be developed, where production of Si–Ge is fully automated. Only then can commercial applications be considered. If additionally the growth of semi-insulating Si–Ge is required, one has to employ crucible-free growth methods, such as float-zone processes. Also pulling from a melt (Czochralski) using quartz crucibles might be possible, but only the float zone method provides a macrosegregation-free ingot without the requirement of adding supplements to the equipment like charging rods, etc. With the existing FZ-technology, which is mainly designed for Si-growth, commercial processing of Si–Ge with compositions down to 80 at % Si should be possible without need for major changes to the equipment.

As far as defects in Si–Ge are concerned, a major source is periodic changes in growth conditions leading to compositional striations, and concomitantly to strain and dislocations due to lattice constant changes. Typical defect densities are found to be in the range 10^4 to 10^7 cm^{-2}. This is the same range as delivered by MBE or CVD layers on Si-substrates, which makes bulk Si–Ge indeed a possible candidate for substrate material. Meanwhile it was shown that the FZ of dislocation free $Si_{0.95}Ge_{0.05}$ is possible [117].

6. Appendix

This additional section outlines possible applications of bulk Si–Ge crystals.

Photodetectors. The positions of impurity levels in the band gap and the band gap energy itself in Si–Ge are a function of composition [99], thus offering the possibility to construct tunable impurity activated photoconductors as well as tunable intrinsic photodetectors [10, 29, 100].

Solar cells. Solid solution Si–Ge crystals in comparison to pure Si have an enhanced sensitivity in the long-wavelength region [101]. Recently it was proposed that solar cells can show an enhanced performance due to Auger generation by carriers excited by photons with energies above the first direct band gap. To match such a device to the solar spectrum, material with a smaller band gap than silicon is required and Si–Ge is assumed to be a promising candidate [102]. Si–Ge is therefore appropriate to enhance the efficiency of a solar cell device not only in the long wavelength but also in the UV region of the solar spectrum.

Functionally graded materials. The Si–Ge solid solution exhibits large differences in a number of physical properties, i.e. the band gap, the lattice constant, the dielectric function, just to name a few. Therefore a gradient in composition shows a local dependence on physical properties [103, 104]. A device based on a gradient in band gap is e.g. a graded gap solar cell or a spectrometer. Change of the dielectric function is employed by gradient index optical devices [105] or dielectric transformer systems for microwave applications. Thermal neutron and X-ray band-pass diffraction crystals [106, 50] are based on a gradient in lattice constant. Lattice spacing changes can also be exploited for designing X-ray focusing systems. Change of thermo-voltage as a function of composition leads to the design of graded thermoelectric devices, which were first mentioned by Joffe [107].

Thermoelectric material. This is probably the most widespread application of Si–Ge [108, 109, 110, 111]. The large difference in mass between the two constituents makes the alloy a poor thermal conductor due to alloy scattering of the phonons. Together with its high thermopower and comparatively large electrical conductivity and low diffusion of the atoms in the lattice, Si–Ge is an excellent thermoelectric material with additionally good mechanical properties for temperatures around 1000 °C. This alloy was chosen for converting heat into electricity in the so-called radioisotope thermoelectric generators (RTGs) used for satellites or in NASA's deep space program.

Substrate material. The lattice constant of Ge-rich Si–Ge can be adjusted to match that of the GaAs or the ZnS compound. Therefore a Si–Ge wafer can potentially be used as alternative substrate material without any lattice mismatch to GaAs structures or ZnS layers. Equally interesting is the use of Si–Ge as substrates for Si–Ge strained layer devices or heterostructures [112]. However, the nonavailability of larger amounts of material to date has impeded work going beyond laboratory experiments.